REDVET - Revista electrónica de Veterinaria - ISSN 1695-7504
Vol 24, No. 4 (2023)
http://www.veterinaria.org
Article Received: Revised: Accepted:

Boundary layer flow of MHD Williamson nano fluid flow over a curved stretching surface

Nagaraju Kasula[1]* and M N Raja Shekar[2]

[1]Department of Mathematics, Sreenidhi Institute of Science and Technology, Yamnampet, Ghatkesar, Hyderabad, Telangana-501 301. India. Email ID: knrnitw@gmail.com
[2]Department of Mathematics, JNTUH UCEJ, Hyderabad, Telangana- 500085. India. Email ID: mnrs71@gmail.com

Abstract:
This study explores the effects of heat and mass transfer on the Williamson nanofluid over a porous exponentially curved stretching sheet is discussed. This analysis is carried out subject to the Brownian motion and thermophoresis. The highly nonlinear partial differential equations are converted into nonlinear ordinary differential equations using similarity transformations and finally solved with the help of finite element method. The results are obtained and good agreement with previous published results of the same nature in the limiting case. The effects of prominent physical parameters like, magnetic field parameter, Brownian motion parameter, thermophoresis parameter, Williamson fluid parameter, Prandtl number and Schmidt number on velocity, temperature and concentration is displayed by using graphs. Numerical results of skin-friction coefficient, Nusselt and Sherwood numbers are systematized in the form of tables.

Keywords: Williamson fluid, MHD, FEM, curved stretching sheet and nanofluid.

1. Introduction:

Sakiadis [1] discussed the study of boundary layer low over a moving solid with constant speed. The study of boundary layer behaviour induced by a stretching sheet is attractive the modern researchers due to it has wide range of applications in engineering processes for example, cooling of an infinite metallic plate in paper production, condensation on n process, tinning of copper wire, etc. Crane [2] initially developed fluid flow due to stretching sheet. It is observed that extensive studies on this topic have been taking on for linear stretching surface. From these studies, the curved surface is not considered. Sajid et al. [3] examined the flow of viscous fluid caused by a curved stretching surface. Okechi et al. [4] reported flow of viscous fluid caused by an exponentially stretching curved surface. Further, recent investigations on curved stretching surface can be quoted through the studies [5-7].
At the present time engineers and researchers have been focused on the analysis of non-Newtonian fluid flows affected by stretching surfaces. This is due to the practical wants in these things in the industry, engineering and technology. Most of the fluids the non-Newtonian materials, which are worked from day to day life. Specific examples include, body lotions, sugar solutions, shampoo, vaccines and mud, etc. Those fluids which obey the Newton's law of viscosity is known as Newtonian fluids, otherwise, they are called as non-Newtonian fluids, in which, the most usually challenged the Williamson fluids. Which have various applications in continuous casting, fiber spinning, manufacturing of space crafts and production of plastic sheets, etc. Williamson [8] initiated the flow of pseudo-plastic materials and also he shown the model equation to introduce the flow of pseudo-plastic fluid results are verified experimentally. Later, Non-Newtonian flow through stretching sheet was studied analytically by Liao [9]. Nadeem and Hussain [10] are explores the study of heat transfer effects on Williamson flow through exponentially porous stretching surface by using optimal homotopy analysis method (OHAM). The flow of Williamson fluid over a stretching sheet was discussed analytically with help of homotopy analysis method by Nadeem and Hussain [11]. Sugunamma et al. [12] explored that simultaneous solution for the flow of Williamson fluid over a curved sheet by shooting technique.

Magneto-fluid-dynamics is a wide-ranging field of research that can be analyse on the dynamical physics of electrically conducting fluids like salt water, plasma and electrolytes. Magnetohydrodynamic is important in numerous uses for example, treatment of some arterial diseases and hyperthermia, reduction of blood during surgeries, magnetic cell separation and drug delivery. Bhatti and Rashidi [13] studied the Williamson nanofluid flow with the effects of thermal radiation and thermo-diffusion over a porous stretching or shrinking sheet. MHD Williamson nanofluid flow over a stretching cylinder with variable thermal conductivity was studied numerically by Bilal et al. [14]. Hayat et al. [15] examined that the MHD flow of second grade nanofluid past a nonlinear stretched surface. Makinde and Aziz [16] illustrated a boundary layer flow of a viscous fluid over a stretched surface by convective heat and mass transfer effects. Rashidi et al. [17] discussed the magnetohydrodynamic flow of fluid owing to a stretching sheet with the buoyancy and thermal radiation effects.

REDVET - Revista electrónica de Veterinaria - ISSN 1695-7504
Vol 24, No. 4 (2023)
http://www.veterinaria.org
Article Received: Revised: Accepted:

Conventional heat transfer base fluids have very poor heat transfer characteristics with low thermal conductivity like, oil, ethylene glycol, water and propylene glycol, etc. Presence of ultrafine nanometer sized particles in the conventional heat transfer fluids remarkably boosts the thermal characteristics of such fluids. Nanofluids have wide range of applications in various biomedical and engineering sectors like coolants of nuclear reactor, cancer therapy, safety problems, micro machines in micro reactors, safer surgeries, cooling agent in air planes, cars, etc. Earlier, Choi [18] familiarized the word nanofluid. He observed that the insertion of metallic nanoparticles in conventional heat transfer fluids enhance the heat transfer and thermal conductivities of such fluids. Later, Buongiorno[19] introduced a mathematical model for convective transport of nanofluid. He established that thermophoresis and Brownian diffusion are most significant slip mechanisms. Waris et al. [20] studied the Williamson nanofluid flow with varying thermal conductivity on time-dependent stretching surface. Hayat et al. [21] studied the hydromagnetic flow of Williamson fluid in thermal radiation and Ohmic viscous dissipation.
Most of the above mentioned articles are studied on Williamson nanofluid on stretching sheet. Not much literature is available for linear curved stretching surface. The main purpose of the present paper is to analyze the effect of magnetohydrodynamic Williamson nanofluid over linear curved stretching surface. Furthermore the Brownian and thermophoresis effects are considered in this article and the solutions for the heat and mass transfer are computed numerically by Finite Element Method.

2. Mathematical Formulations:-

Let us consider the steady two dimensional boundary layer flow of Williamson fluid over a linear curved stretching surface. The flow configuration taking in the direction of u, v and these are the velocity components of s and r - directions respectively. Then s, r are the curved linear coordinates along the sheet and normal to it, R is the radius in between origin to curvature surface and $U_w(x) = as$ is the stretching velocity along the $s-$ direction and a is the nonzero positive constant and the flow chart is shown in Fig.1. The Williamson flow fluid model presents a pseudoplastic or shear thinning properties. The Williamson model has minimum and maximum viscosities of the fluid these are needed for pseudoplastic materials. Williamson discussed the flow of pseudoplastic materials and presented a model equation to analyze the flow of pseudoplastic fluids.
The model of Williamson fluid with extra stress is written as

$$\tau = \left[\mu_\infty + (\mu_0 - \mu_\infty)(1 - \Gamma \dot{\gamma})^{-1} \right] A_1$$

If the value of μ_∞ is zero and μ_0 is equal to μ and the product value of $\Gamma\ddot{\gamma}$ is less than 1 then the model with extra tensor is reduced to

$$\tau = \mu(1 + \Gamma \dot{\gamma}) A_1$$

Where μ_0 indicated zero-shear rate, μ_∞ indicated infinity shear-rate viscous, first Rivlin-Erickson tensor is defined by $A_1 = \nabla \bar{V} + (\nabla \bar{V})^T$, material time constant is defined by Γ and $\dot{\gamma} = \sqrt{\frac{1}{2} tr(A_1)^2}$ is defined as rate of shear and also governing equations are defined as:

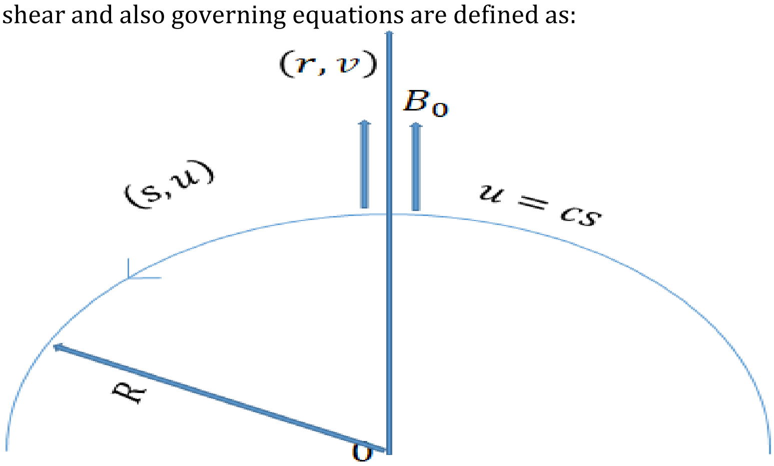

Fig. 1: Geometrical flow.

$$\left(r + R\right) \frac{\partial v}{\partial r} + v + R \frac{\partial u}{\partial s} = 0, \tag{1}$$

REDVET - Revista electrónica de Veterinaria - ISSN 1695-7504
Vol 24, No. 4 (2023)
http://www.veterinaria.org
Article Received: Revised: Accepted:

$$\frac{\partial P}{\partial r}=\frac{\rho}{r+R}u^2 \quad (2)$$

$$v\frac{\partial u}{\partial r}+\frac{Ru}{r+R}\frac{\partial u}{\partial s}+\frac{uv}{r+R}=-\frac{1}{\rho}\frac{R}{r+R}\frac{\partial P}{\partial s}$$
$$+\frac{\mu}{\rho}\left(1+\sqrt{2}\Gamma\left(\frac{\partial u}{\partial r}-\frac{1}{r+R}u\right)\right)\left(\frac{\partial^2 u}{\partial r^2}+\frac{1}{r+R}\frac{\partial u}{\partial r}-\frac{1}{(r+R)^2}u\right)-\frac{\sigma B_0^2}{\rho}u \quad (3)$$

$$v\frac{\partial T}{\partial r}+\frac{Ru}{r+R}\frac{\partial T}{\partial s}=\alpha\left(\frac{\partial^2 T}{\partial r^2}+\frac{1}{r+R}\frac{\partial T}{\partial r}\right)+\frac{(\rho c)_p}{(\rho c)_f}\left(D_B\left(\frac{\partial C}{\partial r}\frac{\partial T}{\partial r}\right)+\frac{D_T}{T_\infty}\left(\frac{\partial T}{\partial r}\right)^2\right) \quad (4)$$

$$v\frac{\partial C}{\partial r}+\frac{Ru}{r+R}\frac{\partial C}{\partial s}=D_B\left(\frac{\partial^2 C}{\partial r^2}+\frac{1}{r+R}\frac{\partial C}{\partial r}\right)+\frac{D_T}{T_\infty}\left(\frac{\partial^2 T}{\partial r^2}+\frac{1}{r+R}\frac{\partial T}{\partial r}\right) \quad (5)$$

With boundary conditions are:

$$u=U_w(s)=cs,\ v=0,\ T=T_w,\ D_B\frac{\partial C}{\partial r}+\frac{D_T}{T_\infty}\frac{\partial T}{\partial r}=0 \text{ at } r=0 \quad 6(a)$$

$$u\to 0,\ \frac{\partial u}{\partial r}\to 0,\ T\to T_\infty,\ C\to C_\infty \text{ at } r\to\infty \quad 6(b)$$

Here velocity U_w, temperature T_w and concentration C_w are near at the wall. The temperature T_∞ and concentration C_∞ are away the surface and kinematic viscosity is $v=\mu/\rho_f$, the density parameter is ρ_f, the dynamic viscosity μ, the thermal diffusivity of the fluid parameter is $\alpha=k/(\rho c)_f$, the thermal conductivity is k, the heat capacity of fluid is $(\rho c)_f$, the diffusion coefficient is D_T, the Brownian diffusivity coefficient is D_B. In order to get the non-dimensional form of the nonlinear partial differential equations are converting into the nonlinear ordinary differential equations using the following suitable similarity transformations

$$\eta=r\sqrt{c/\upsilon},\ P=\rho c^2 s^2 P(\eta),\ u=csf'(\eta),$$
$$v=-\frac{R}{r+R}\sqrt{c\upsilon}f(\eta),\ \theta(\eta)=\frac{T-T_\infty}{T_f-T_\infty},\phi(\eta)=\frac{C-C_\infty}{C_f-C_\infty}. \quad (7)$$

Here, identically satisfied the equation (1) and other equations (2)-(7) are given bellow:

$$\frac{\partial P}{\partial \eta}=\frac{f'^2}{\eta+K} \quad (8)$$

$$\frac{2K}{\eta+K}P(\eta)=\left(1+\lambda\left(f''-f'\right)\right)\left(f'''+\frac{1}{\eta+K}f''-\frac{1}{(\eta+K)^2}f'\right)+\frac{K}{\eta+K}\left(ff''-f'^2\right)$$
$$+\frac{K}{(\eta+K)^2}ff'-Mf' \quad (9)$$

$$\theta''+\frac{1}{\eta+K}\theta'+\frac{K}{(\eta+K)}\Pr f\theta'+\Pr Nb\phi'\theta'+\Pr Nt\theta'^2=0 \quad (10)$$

$$\phi''+\frac{1}{\eta+K}\phi'+\frac{Nt}{Nb}\left(\theta''+\frac{1}{\eta+K}\theta'\right)+\frac{K}{(\eta+K)}Scf\phi'=0 \quad (11)$$

The connected non-dimensional boundary conditions are

$$\left\{\begin{matrix} f(\eta)=0,\ f'(\eta)=1,\ \theta(\eta)=1, Nb\phi'(\eta)+Nt\theta'(\eta)=0 \ \ at\ \eta=0, \\ f'(\eta)=0,\ f''(\eta)=0,\ \theta(\eta)=0,\ \phi(\eta)=0,\ \ as\ \ \eta\to\infty \end{matrix}\right\} \quad (12)$$

REDVET - Revista electrónica de Veterinaria - ISSN 1695-7504
Vol 24, No. 4 (2023)
http://www.veterinaria.org
Article Received: Revised: Accepted:

Where some of non-dimensional parameters associated as, the curvature parameter is $K = R\sqrt{c/\upsilon}$, the magnetic parameter is $M = \left(\frac{\sigma B_0^2}{\rho c}\right)$, the Williamson fluid parameters is $\lambda = \Gamma\left(\frac{2c^3}{\upsilon}\right)^{1/2} s$, the Prandtl number is $\Pr = \upsilon/\alpha$, the Brownian motion parameter is $Nb = \frac{(\rho c)_p D_B}{(\rho c)_f \upsilon}(C_f - C_\infty)$, the thermophoresis parameter is $Nt = \frac{(\rho c)_p D_T}{(\rho c)_f \upsilon T_\infty}(T_f - T_\infty)$, and the Schmidt number is $Sc(=\upsilon/D_B)$.

Now reducing pressure P from equations (9) and (10), we get

$$\left(1+\lambda\left(f''-f'\right)\right)\left(f^{IV}+\frac{2}{\eta+K}f'''-\frac{1}{(\eta+K)^2}f''+\frac{1}{(\eta+K)^3}f'\right)+\lambda\left(f'''-f''\right)$$
$$\left(f'''+\frac{1}{\eta+K}f''-\frac{1}{(\eta+K)^2}f'\right)+\frac{K}{\eta+K}\left(ff'''-f'f''\right)+\frac{K}{(\eta+K)^2}ff'' \tag{13}$$
$$-\frac{K}{(\eta+K)^3}ff'-\frac{K}{(\eta+K)^2}f'^2-M\left(f''+\frac{1}{\eta+K}f'\right)=0$$

Pressure P can be calculated from equations (10) as:

$$P(\eta)=\left(\frac{\eta+K}{2K}\right)\left\{\left(1+\lambda\left(f''-f'\right)\right)\left(f'''+\frac{1}{\eta+K}f''-\frac{1}{(\eta+K)^2}f'\right)+\frac{K}{\eta+K}\left(ff''-f'^2\right)\right\}$$
$$+\left(\frac{\eta+K}{2K}\right)\left\{\frac{K}{(\eta+K)^2}ff'-Mf'\right\} \tag{15}$$

For the engineering purpose using of physical quantities are skin friction coefficient (C_f), local Nusselt number (Nu) and Sherwood number (Sh) are

$$C_f=\frac{\tau_f}{(1/2)\rho U_w^2},\ Nu=\frac{sq_w}{k_f(T_f-T_\infty)},\ Sh=\frac{sh_m}{D_m(C_f-C_\infty)} \tag{16}$$

Where stands for wall shear stress and heat flux are expressed as.

$$\tau_f=\mu\left(\left[\frac{\partial u}{\partial r}-\frac{u}{r+R}\right]+\frac{\Gamma}{\sqrt{2}}\left[\frac{\partial u}{\partial r}-\frac{u}{r+R}\right]^2\right)_{r=0},\quad q_w=-k_f\left(\frac{\partial T}{\partial r}\right)_{r=0},\quad h_m=-D_m\left(\frac{\partial C}{\partial r}\right)_{r=0} \tag{17}$$

The non-dimensional skin fraction coefficient (C_f), local Nusselt number (Nu) and Sherwood number (Sh) are:

$$\frac{1}{2}C_f\left(\mathrm{Re}_x\right)^{1/2}=\left[\left(f''(0)-\frac{1}{K}f'(0)\right)+\frac{\lambda}{2}\left(f''(0)-\frac{1}{K}f'(0)\right)^2\right],$$
$$Nu\left(\mathrm{Re}_s\right)^{-1/2}=-\theta'(0),\ Sh\left(\mathrm{Re}_x\right)^{-1/2}=-\phi'(0) \tag{18}$$

Here $\mathrm{Re}_s = cs^2/\upsilon$ stands for local Reynolds number.

3. Results and discussions:

We solved Eqs. (5.2.11) - (5.2.13) with respect to their boundary condition (5.2.14) by using of Runge-Kutta-Felburg with shooting technique. The influence of physical parameters connected Williamson flow parameter (λ), magnetic parameter (M), curvature parameter (K), Brownian parameter (Nb), thermophorasis parameter (Nt) and Schmidt number (Sc) on velocity, temperature and concentration profiles. Here computation purposes fixing the values of physical parameter as

$M = 0.2, \lambda = 0.03, K = 5, Nb = 0.3, Nt = 0.6, Sc = 10$. In this conversation of whole values becomes a constant excluding for the difference is expressed in the graphs.

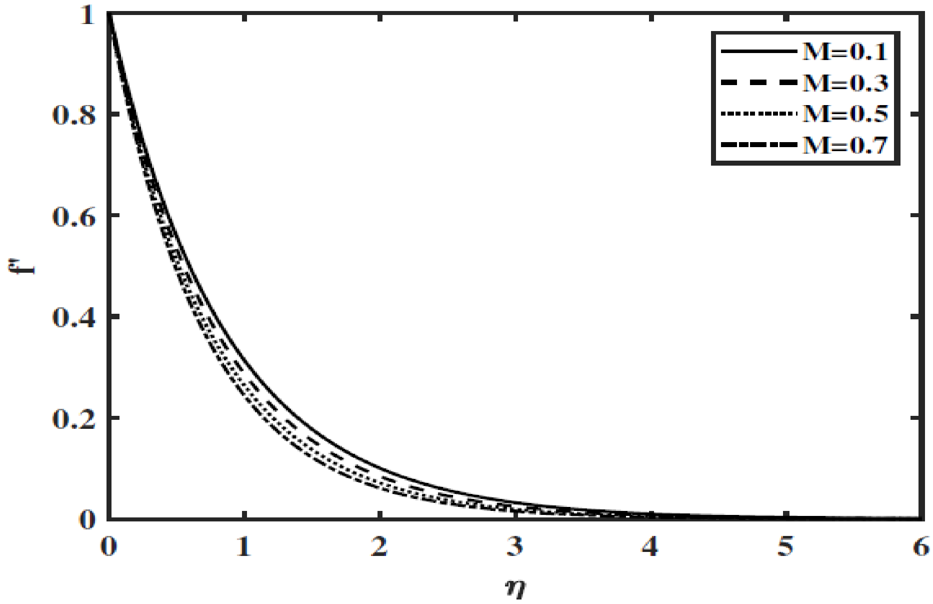

Fig. 2 Influence of magnetic parameter $(M = 0.1, 0.3, 0.5, 0.7)$ **on velocity profile.**

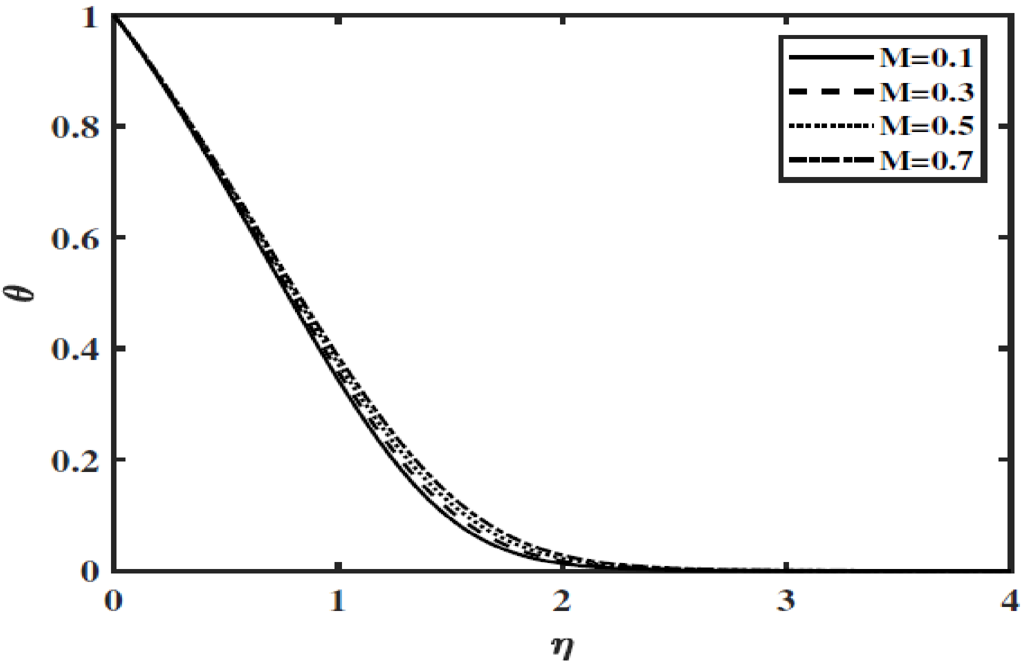

Fig. 3 Influence of magnetic parameter $(M = 0.1, 0.3, 0.5, 0.7)$ **on temperature profile.**

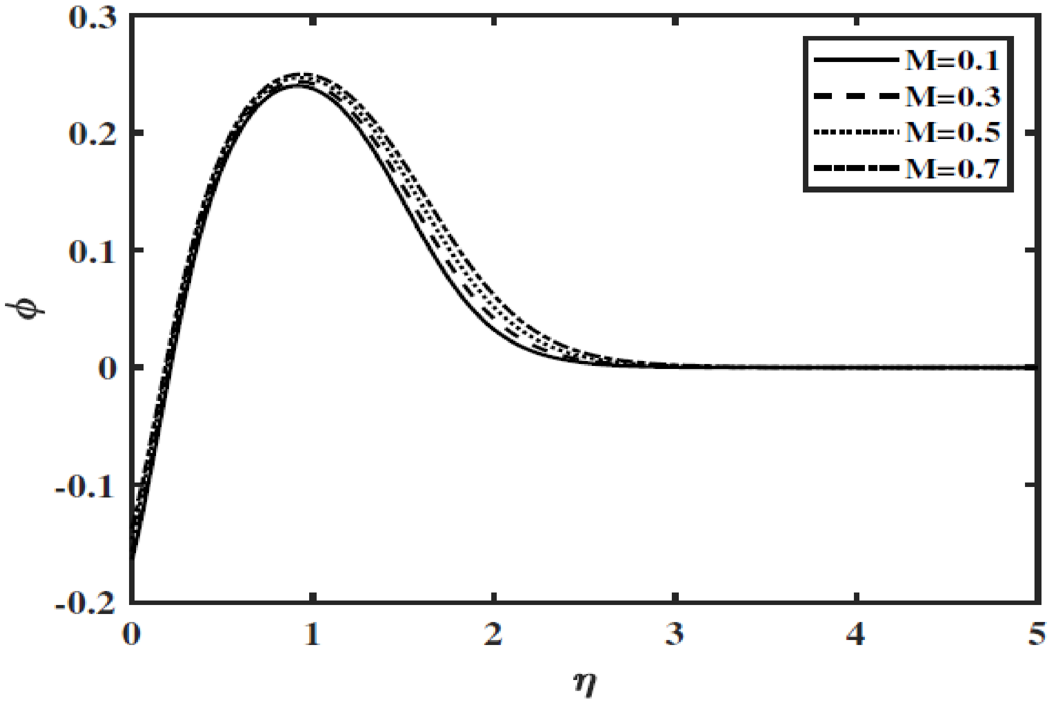

Fig. 4. The impact of magnetic parameter $(M = 0.1, 0.3, 0.5, 0.7)$ on concentration profile.

Fig. 2 shows the difference of the velocity profile with magnetic parameter $(M = 0.1, 0.3, 0.5, 0.7)$. That is the velocity profile reductions with the rises of magnetic parameter M. This is shows the fluid velocity profile has been decline by rising in the magnetic field. Here the velocity boundary layer thickness is thinner as magnetic parameter. This is due to the fact the application of a magnetic field to an electrically conducting fluid yields as a drag force which causes decline in the fluid velocity. Fig. 3 illustrates the influence of magnetic parameter $(M = 0.1, 0.3, 0.5, 0.7)$ on temperature profile. From this figure observed that the temperature profile enhances with enhanced magnetic parameter M. That is the reason for the effect of increased Lorentz force on temperature. The impact of magnetic parameter $(M = 0.1, 0.3, 0.5, 0.7)$ are shown in Fig. 4, which shows that an enhanced concentration profile with enhanced magnetic parameter.

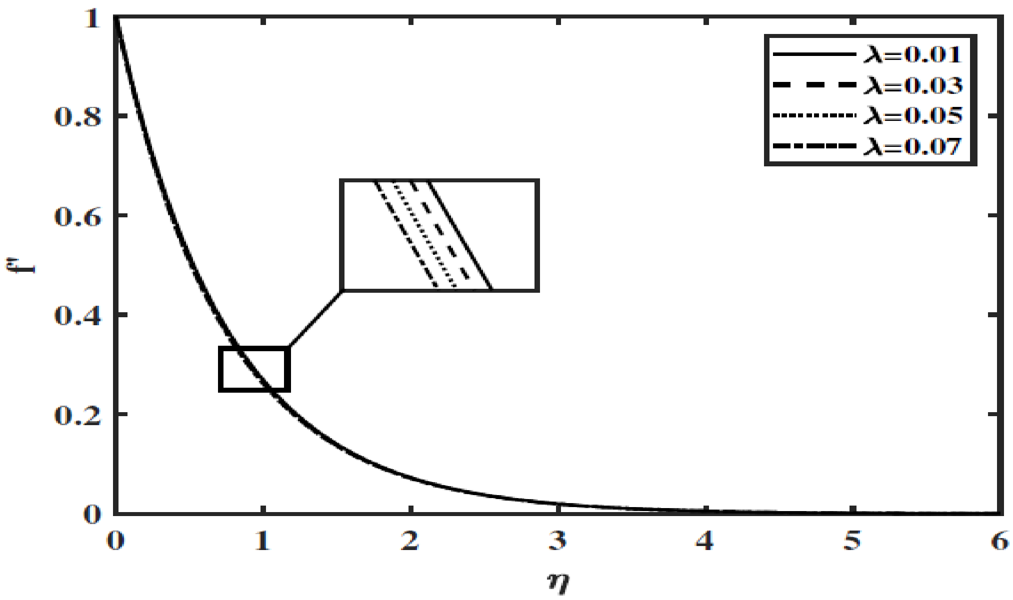

Fig. 5. The effect of Williamson fluid parameter $(\lambda = 0.01, 0.03, 0.05, 0.07)$ on dimensionless velocity profile.

REDVET - Revista electrónica de Veterinaria - ISSN 1695-7504
Vol 24, No. 4 (2023)
http://www.veterinaria.org
Article Received: Revised: Accepted:

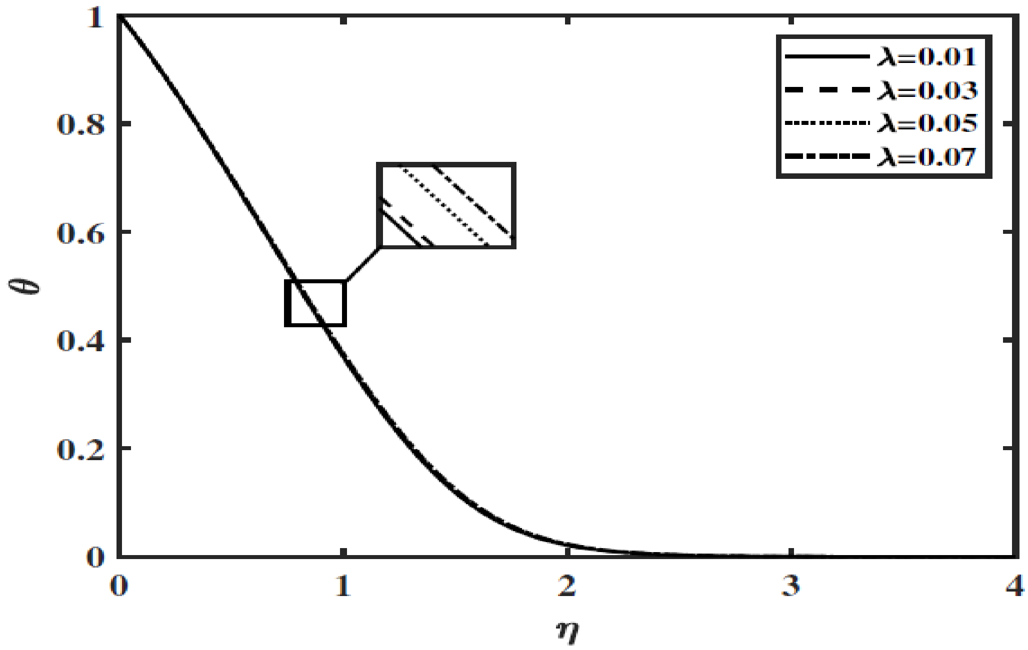

Fig. 6. The effect of Williamson fluid parameter $(\lambda = 0.01, 0.03, 0.05, 0.07)$ **on dimensionless temperature profile.**

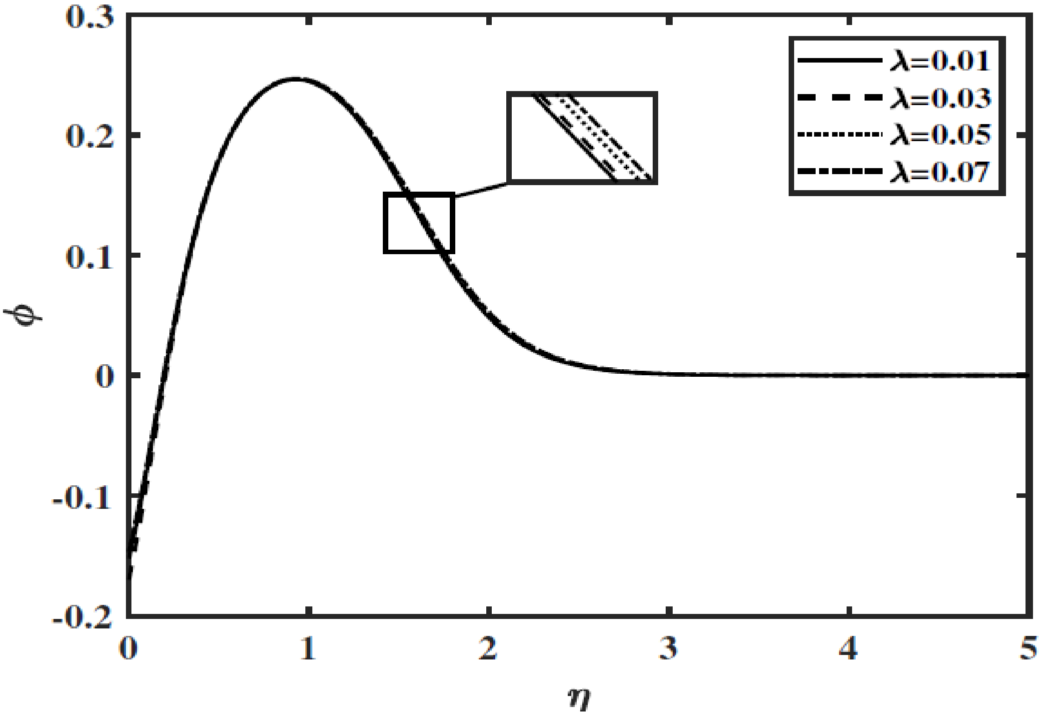

Fig. 7. The effect of Williamson fluid parameter $(\lambda = 0.01, 0.03, 0.05, 0.07)$ **on dimensionless concentration profile.**

REDVET - Revista electrónica de Veterinaria - ISSN 1695-7504
Vol 24, No. 4 (2023)
http://www.veterinaria.org
Article Received: Revised: Accepted:

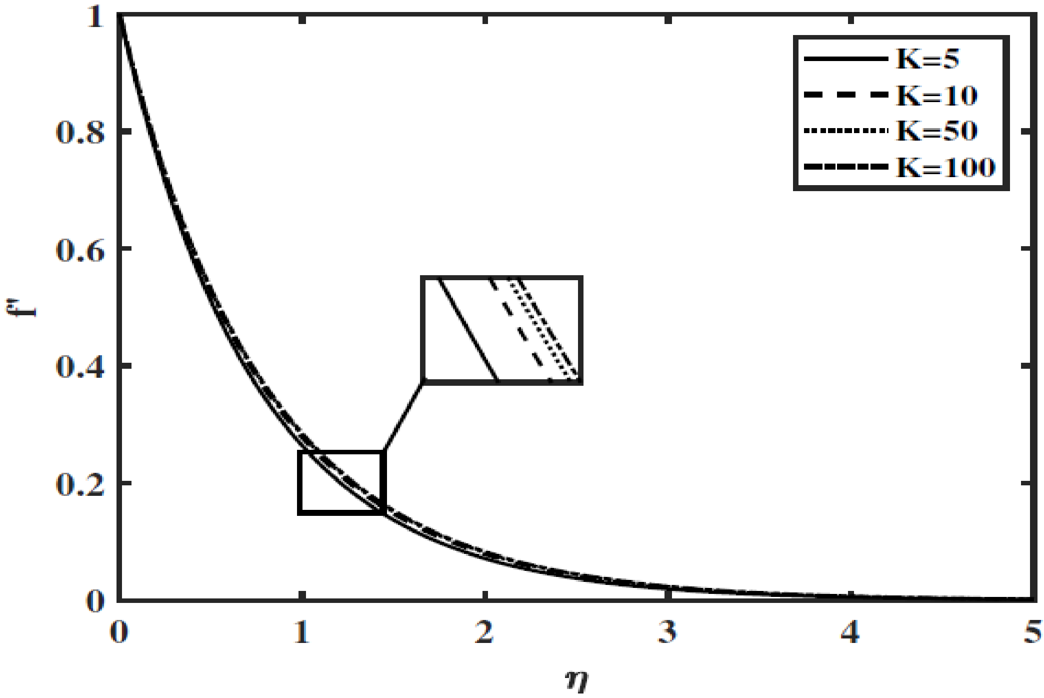

Figs. 8. Influence of curvature parameter $(K = 5,10,50,100)$ **on dimensionless velocity profile.**

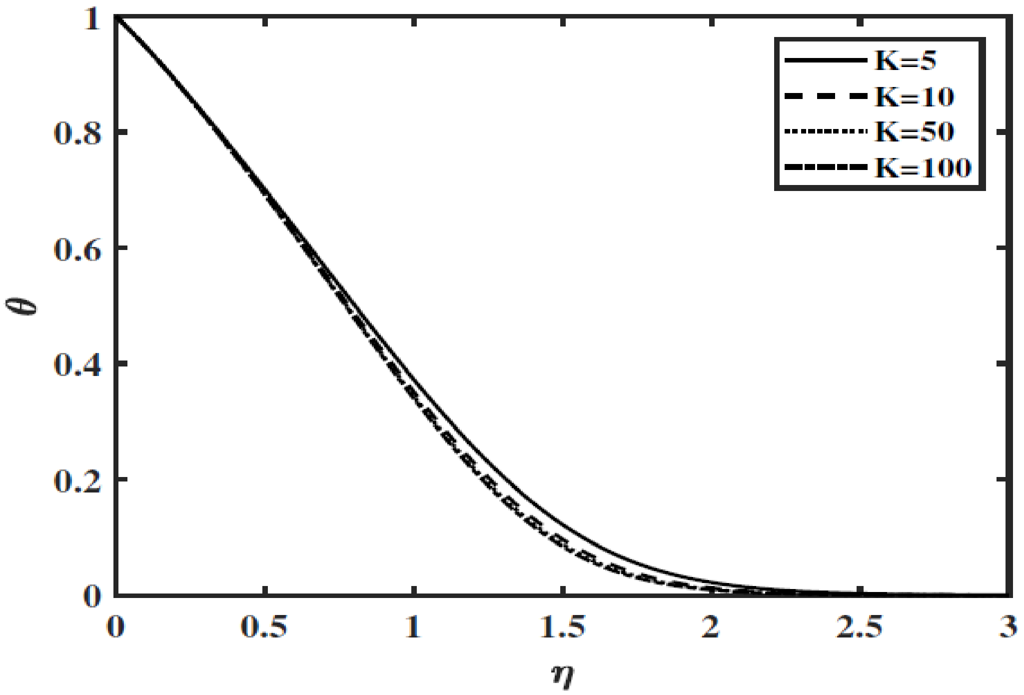

Figs. 9. Influence of curvature parameter $(K = 5,10,50,100)$ **on dimensionless temperature profile.**

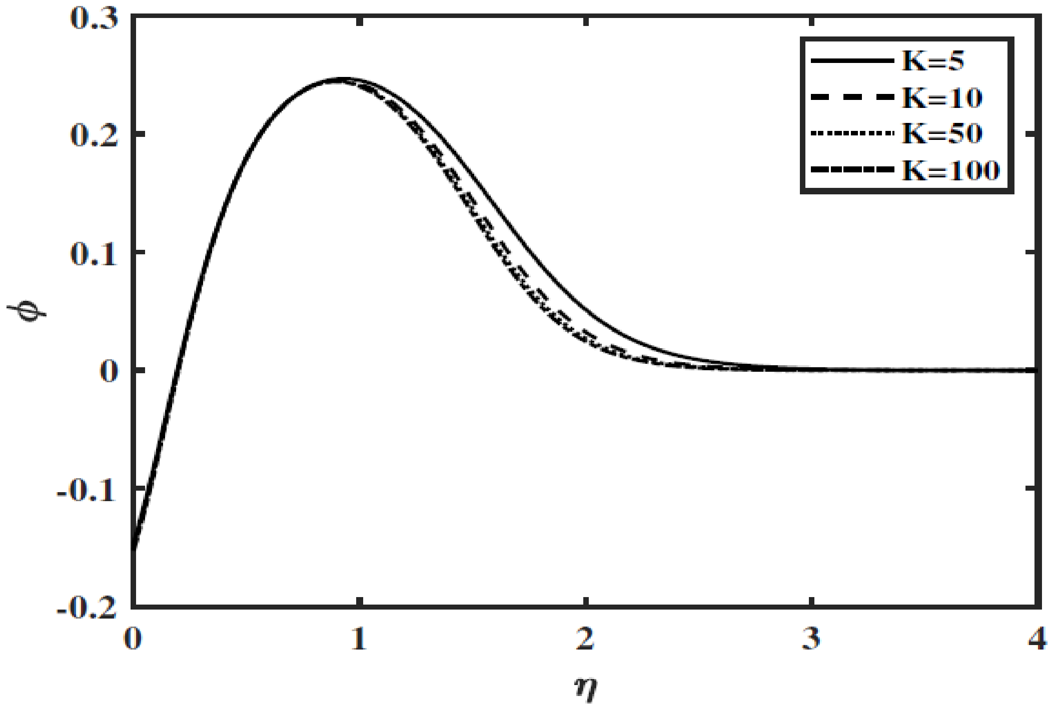

Figs. 10. Influence of curvature parameter $(K = 5, 10, 50, 100)$ **on dimensionless concentration profile.**

The effect of Williamson fluid parameter $(\lambda = 0.01, 0.03, 0.05, 0.07)$ on dimensionless velocity, temperature and concentration profiles by using other parameters are fixed and represented in Figs. 5-7. From these Figs., we obtained that the velocity profile decreases while temperature and concentration profiles increases by enhancing the values of Williamson fluid parameter.

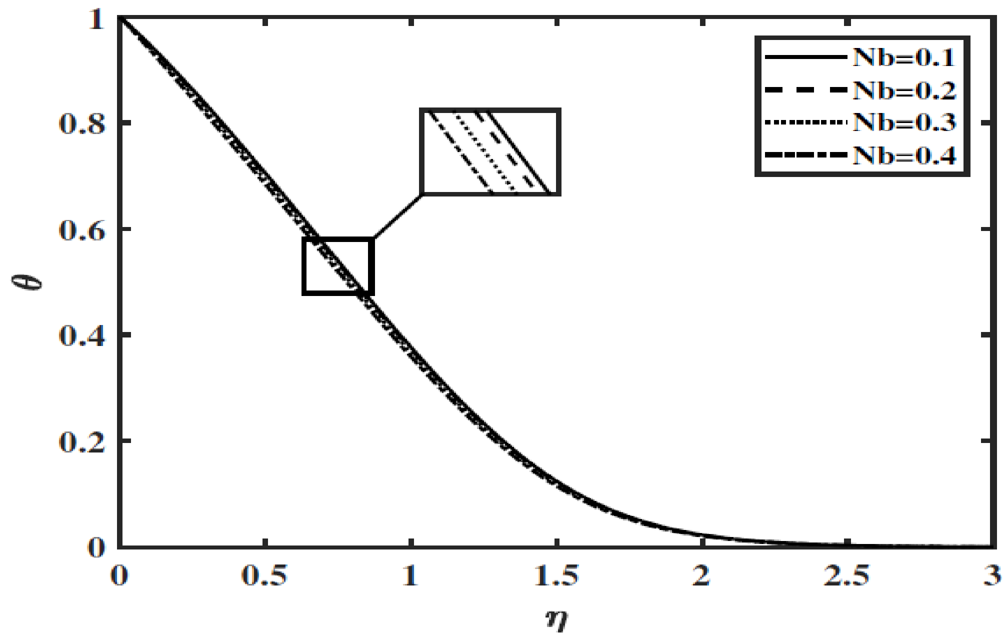

Fig. 11 The Brownian motion parameter $(Nb = 0.1, 0.2, 0.3, 0.4)$ **impact on temperature profile.**

REDVET - Revista electrónica de Veterinaria - ISSN 1695-7504
Vol 24, No. 4 (2023)
http://www.veterinaria.org
Article Received: Revised: Accepted:

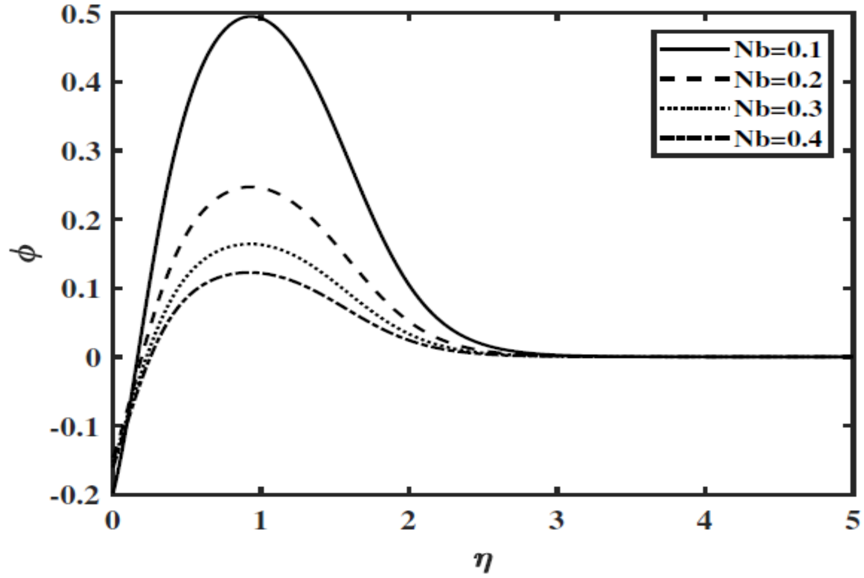

Fig.12 The Brownian motion parameter $(Nb = 0.1, 0.2, 0.3, 0.4)$ **impact on concentration profile.**

Figs. 8-10 indicates influence of curvature parameter $(K = 5, 10, 50, 100)$ on dimensionless velocity, temperature and concentration profiles. It is shown that the velocity profile is enhancing and temperature, concentration profiles are declining function of curvature parameter.

Fig. 11 and 12 describes the Brownian motion parameter $(Nb = 0.1, 0.2, 0.3, 0.4)$ impact on temperature and concentration profiles. Here found that the raised values of Brownian motion parameter in the temperature is decreases in branches of solutions (Fig. 11). For the concentration profile reverse influence is noticed. i.e. concentration profile decline with the enhances of Brownian motion parameter for branches of solution (Fig. 12). So, the concentration profile is significantly affected by the rises of Brownian motion parameter.

In Figs. 13 and 14 due to impacts of thermophoresis parameter $(Nt = 0.2, 0.4, 0.6, 0.8)$ on temperature and concentration profiles are represented. Due to enhanced values of thermophoresis parameter, for both the cases of temperature (Fig. 13) and concentration (Fig. 14) profiles are increases. In nanofluidthermophorasis parameter defines as the ratio of nanoparticle diffusion to the thermal diffusion. Due to enhance in Nt the temperature variance between the curved sheet and fluid enhances and thermal boundary layer enhances in this case. In nanofluid, the thermophorasis force enhances which helps the nanoparticle to move from hot region to cold region. That is the movement of **concentration profile rises.**

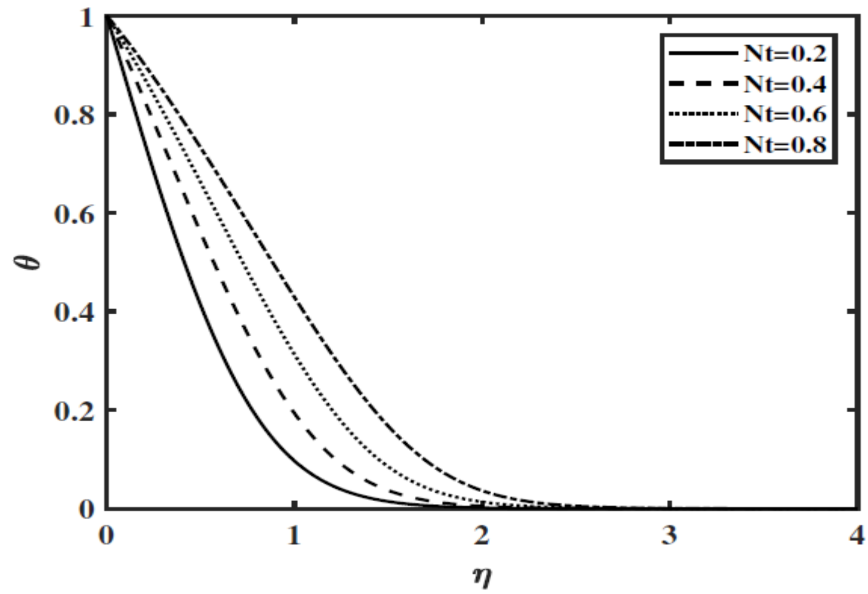

Fig. 13 Impacts of thermophoresis parameter $(Nt = 0.2, 0.4, 0.6, 0.8)$ **on temperature profile.**

REDVET - Revista electrónica de Veterinaria - ISSN 1695-7504
Vol 24, No. 4 (2023)
http://www.veterinaria.org
Article Received: Revised: Accepted:

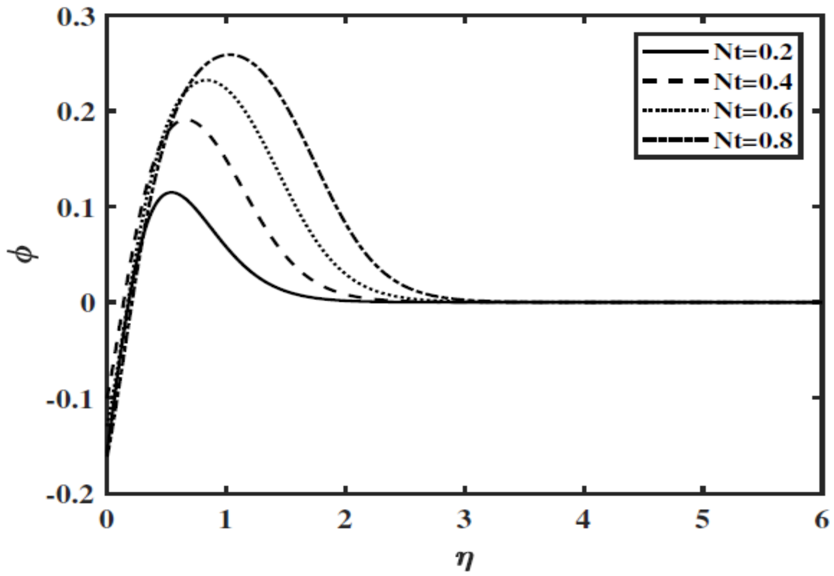

Fig. 14 Impacts of thermophoresis parameter $(Nt = 0.2, 0.4, 0.6, 0.8)$ **on concentration profile.**

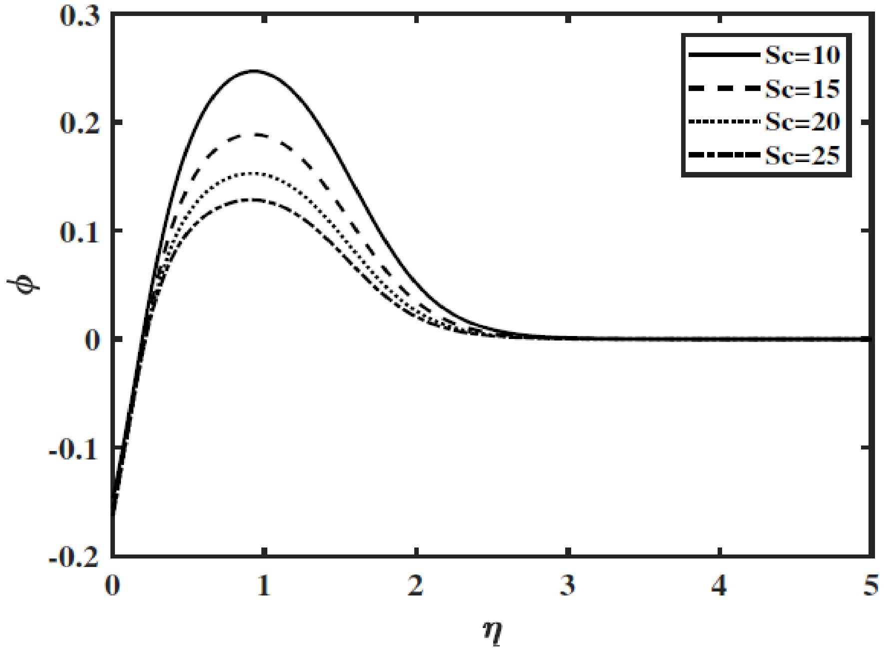

Fig. 15 Impact of large values of Schmidt number $(Sc = 10, 15, 20, 25)$ **on concentration profile.**

Fig. 15 displays the impact of large values of Schmidt number $(Sc = 10, 15, 20, 25)$ on concentration profile. The behavior of Schmidt number as inversely proportional to the mass diffusion so enhancing Schmidt number Sc illustrates decline in concentration profile and its linked thickness of boundary layer.

Conclusions:

In these article, we observed that the effect of Brownian motion on MHD boundary layer flow of Williamson nanouid over a curved stretching surface with flexible thermal conductivity and thickness is existing. The governed equations are converted in to the consisting ordinary differential equations by utilizing the suitable similarity transforms. These ordinary differential equations were further solved numerically by Runge-Kutta-Felburg with shooting method. From the numerical valuesare acquired, some of interested key pointes are given following:

- Velocity profile decline while temperature and concentration profiles are improving by enhanced values of Williamson fluid parameter (λ).

- Enhancing magnetic parameter decline the velocity $(f'(\eta))$ profile whereas enhances temperature $(\theta(\eta))$ and concentration $(\phi(\eta))$ profiles.
- Velocity $(f'(\eta))$ is enhancing, temperature $(\theta(\eta))$ and concentration $(\phi(\eta))$ are declining with effect of curvature parameter.
- Enhanced values of thermophoresis parameter (Nt), for the both cases of temperature and concentration profiles are increases.

CRediT authorship contribution statement:

Nagaraju Kasula: Writing – original draft, Methodology. Conceptualization, Writing – original draft, Software.
M N Raja Shekar: Supervision, Conceptualization, Writing – review & editing.

Declaration of competing interest:
The authors declare that they have no known competing financial interests or personal relationships that could have appeared to influence the work reported in this paper.

Availability of data and materials: Not applicable.
Acknowledgments: The first author sincerely acknowledges JNTUH UCEJ, **Hyderabad,** for their encouragement and institutional support throughout the completion of this work.

References:
[1] Sakiadis BC. Boundary layer behaviour on continuous solid surfaces: Boundary layer equations for two-dimensional and axisymmetric flow. AIChE, 7, (1961), 26-28.
[2] Crane LJ. Flow past a stretching plate, ZAMP, 21, (1970), 645-647.
[3] Sajid M, Ali N, Javed T, Abbas Z. Stretching a curved surface in a viscous fluid. Chinese Physics Letters, 27, (2010), 024703.
[4] Okechi NF, Jalil M, Asghar S. Flow of viscous fluid along an exponentially stretching curved surface. Results in Physics, 7, (2017), 2851-2854.
[5] Hayat T, Saif RS, Ellahi R, Muhammad T, Ahmad B. Numerical study of boundary-layer flow due to a nonlinear curved stretching sheet with convective heat and mass conditions. Results in Physics, 7, (2017), 2601-2606.
[6] T, Rashid M, Imtiaz M, Alsaedi A. MHD convective flow due to a curved surface with thermal radiation and chemical reaction. Journal of Molecular Liquids, 225, (2017), 482-489.
[7] N.F. Okechi, M. Jalil, S. Asghar, Flow of viscous fluid along an exponentially stretching curved surface, Results in Physics, 7, (2017), 2851-2854.
[8] Williamson, R.V., The flow of pseudoplastic materials. Industrial and Engineering Chemistry Research, 21, No. 11, 1108 (1929).
[9] Liao, S.J., On the analytic solution of magnetohydrodynamic flows of non-Newtonian fluids over a stretching sheet, Journal of Fluid Mechanics, 488, (2003), 189-212.
[10] Nadeem, S, Hussain, S.T., Heat transfer analysis of Williamson fluid over exponentially stretching surface, Appl. Math. Mech.35, (2014), 489-502.
[11] Nadeem, S., Hussain, S.T., Lee, C., Flow of Williamson fluid over a stretching sheet, Braz. J. Chem. Eng., 30, (2013), 619-625.
[12] K. Anantha Kumar, J.V. Ramana Reddy, V. Sugunamma, N. Sandeep, Simultaneous solutions for MHD flow of Williamson fluid over a curved sheet with non-uniform heat source/sink, Heat Transfer Research, 50, (2019), 581-603.
[13] M.M. Bhatti, M.M. Rashidi, Effects of thermo-diffusion and thermal radiation on Williamson nanofluid over a porous shrinking/stretching sheet, J. Mol. Liq. 221 (2016) 567-573.
[14] M. Bilal, M. Sagheer, S. Hussain, Numerical study of magneto hydrodynamics and thermal radiation on Williamson nanofluid flow over a stretching cylinder with variable thermal conductivity, Alexandria Engineering Journal, 57, (2018), 3281-3289.
[15] T. Hayat, A. Aziz, T. Muhammad and B. Ahmad, Onmagnetohydrodynamic flow of second grade nanofluid over a nonlinear stretching sheet, J. Magn. Magn. Mater. 408 (2016) 99-106.
[16] O. D. Makinde and A. Aziz, Boundary layer flow of a nanofluid past a stretching sheet with a convective boundary condition, Int. J. Ther. Sci. 50 (2011) 1326-1332.
[17] M. M. Rashidi, N. V. Ganesh, A. K. A. Hakeem and B. Ganga, Buoyancy effect on MHD flow of nanofluid over a stretching sheet in the presence of thermal radiation, J. Mol. Liq. 198 (2014) 234-238.
[18] S.U.S. Choi, Enhancing Thermal Conductivity of Fluids with Nanoparticles, ASME, USA, (1995).

[19] J. Buongiorno, Convective transport in nanofluids, ASME J.Heat Tran. 128 (2006) 240–250.
[20] Waris, K.; Gul, T.; Idrees, M.; Islam, S.; Khan, I.; Dennis, L. Thin film Williamson nanofluid flow with varying viscosity and thermal conductivity on a time-dependent stretching sheet, Appl. Sci. 6, (2016), 334.
[21] T. Hayat, A. Shafiq, A. Alsaedi, Hydromagnetic boundary layer flow of Williamson fluid in the presence of thermal radiation and Ohmic dissipation, Alex. Engr. J. 6 (2016) 035101.